Plug-and-Play Fluorophores Extend the Spectral Properties of Spinach

Wenjiao Song, Rita L. Strack, Nina Svensen, and Samie R. Jaffrey*

Department of Pharmacology, Weill Medical College, Cornell University, New York, New York 10065, United States

ⓢ *Supporting Information*

ABSTRACT: Spinach and Spinach2 are RNA aptamers that can be used for the genetic encoding of fluorescent RNA. Spinach2 binds and activates the fluorescence of (Z)-4-(3,5-difluoro-4-hydroxybenzylidene)-1,2-dimethyl-1H-imidazol-5(4H)-one (DFHBI), allowing the dynamic localizations of Spinach2-tagged RNAs to be imaged in live cells. The spectral properties of Spinach2 are limited by DFHBI, which produces fluorescence that is bluish-green and is not optimized for filters commonly used in fluorescence microscopes. Here we characterize the structural features that are required for fluorophore binding to Spinach2 and describe novel fluorophores that bind and are switched to a fluorescent state by Spinach2. These diverse Spinach2−fluorophore complexes exhibit fluorescence that is more compatible with existing microscopy filter sets and allows Spinach2-tagged constructs to be imaged with either GFP or YFP filter cubes. Thus, these "plug-and-play" fluorophores allow the spectral properties of Spinach2 to be altered on the basis of the specific spectral needs of the experiment.

Imaging RNA in living cells is important for understanding the function and regulation of diverse classes of cellular RNAs. A strategy for imaging RNAs is to express RNAs with sequence tags that confer fluorescence to the RNA.[1] These tags include sequences that recruit GFP.[2] A related approach involves the use of two sequence tags to template the formation of GFP from each half of split GFP.[3] An alternate strategy is to use RNA sequences that exhibit fluorescence upon binding small molecules. Several RNA aptamers that bind and switch on the fluorescence of various small molecule dyes have been described.[4] The use of these dyes is limited because their fluorescence is nonspecifically activated by cellular components.[5] A recent approach to overcome this problem uses RNA aptamers that bind and induce the fluorescence fluorophores resembling those in GFP.[5] The brightest of these RNA−fluorophore complexes are Spinach and a recently improved variant, Spinach2, which exhibits improved folding and thermostability.[5,6] Because these fluorophores exhibit low background fluorescence when incubated with cells, the dynamics of RNA localization in cells can be imaged by engineering cells to express Spinach2 fused to target RNA molecules of interest.[5,6]

Tagging an RNA with Spinach for fluorescent imaging requires identification of an insertion site in the target RNA that is compatible with Spinach folding. Spinach folding can be inhibited by neighboring flanking sequences, presumably due to hybridization interactions that prevent Spinach folding.[6] Researchers may therefore need to screen multiple insertion sites in the target RNA to identify one in which the aptamer can fold efficiently. Furthermore, experiments are needed to confirm that the function of the target RNA is not inhibited by the aptamer. In the case of 5S, 7SK, CGG-repeat toxic RNAs and various bacterial mRNAs, insertion sites have already been identified that tolerate Spinach and/or Spinach2.[5−7] These RNAs interact with (Z)-4-(3,5-difluoro-4-hydroxybenzylidene)-1,2-dimethyl-1H-imidazol-5(4H)-one (DFHBI) to produce a bluish-green fluorescence emission (501 nm) after excitation at 447 nm. Because of the complexity of finding an insertion site in an RNA for Spinach, it would be desirable to not have to reoptimize the RNA for a different aptamer tag in order to perform experiments requiring different fluorescence excitation and/or emission properties.

A limitation of Spinach2 is that it has suboptimal spectral characteristics for fluorescence imaging using standard widefield microscopes. Spinach and Spinach2 bound to DFHBI have fluorescence excitation maxima of 447 nm and peak fluorescence emission of 501 nm.[5,6] These wavelengths do not fully match the filter cubes used for imaging green fluorescence on most microscopes. Typically, these are optimized to detect GFP or fluorescein isothiocyanate, and have a bandpass excitation filter that transmits light at 480 ± 20 nm, a dichroic mirror set at 505 nm, and an emission filter that transmits light at 535 ± 20 nm. As a result, Spinach2−DFHBI complexes are exposed to excitation light that does not lead to maximum fluorescence. Additionally, a considerable portion of the emitted light from Spinach2−DFHBI is not collected since it is blocked by the dichroic mirror or emission filter.
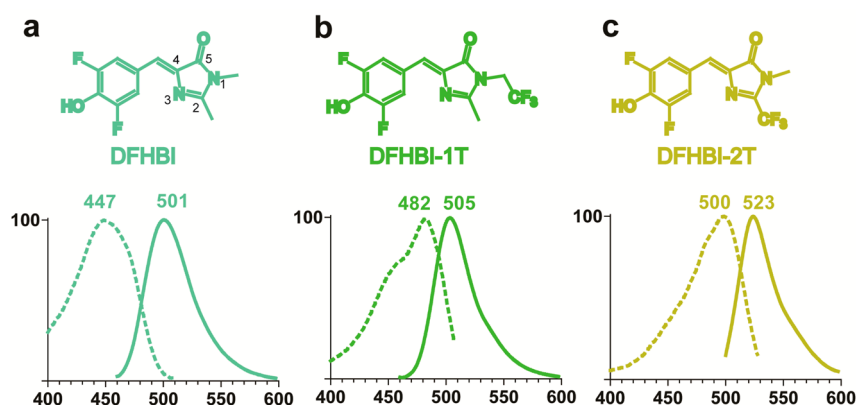
Although we have described other RNA−fluorophore complexes with different excitation and emission maxima, these are not as bright and not optimized to have the same efficient folding as Spinach2.[5,6] Thus, improved and/or novel spectral properties of Spinach2−fluorophore complexes could significantly enhance RNA imaging.

We considered the possibility that modifications to DFHBI could red-shift the excitation and emission properties of the Spinach2−fluorophore complex. To test this idea, we first sought to understand the structural features of DFHBI that are required for Spinach2 to activate its fluorescence. We first examined the role of substituents on the benzylidene ring. Spinach2 tolerated fluorophores containing different halogens
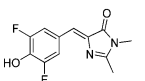
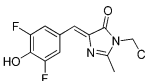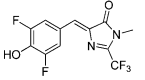**Figure 1.** Different fluorophores bind Spinach2 and form RNA—fluorophore complexes with unique spectral properties. Excitation (dotted line) and emission (solid line) spectra of Spinach2—fluorophore complexes. Excitation and emission spectra were collected in the presence of excess Spinach2 (5 μM) in the presence of different fluorophores (1 μM) in binding buffer (40 mM HEPES, pH 7.4, 125 mM KCl, 10 mM $MgCl_2$): (a) DFHBI, (b) DFHBI-1T, and (c) DFHBI-2T. Spectra are shown as the percent of the maximum excitation and emission fluorescence for each Spinach2—fluorophore complex. Excitation spectra were collected at the indicated emission maximum wavelength, and emission spectra were collected at the indicated excitation-maximum wavelength. The numbering in (a) indicates the atom numbering scheme for the imidazolone ring.

Table 1. Photophysical and Binding Properties of Fluorophore-Spinach2 Complexes

	Fluorophore	Excitation maximum (nm)	Emission maximum (nm)	Extinction coefficient ($M^{-1}cm^{-1}$)[a]	Fluorescence quantum yield	K_D (nM)	Brightness[b]
	DFHBI	423	489	30,100	0.0007	-	0.13
	Spinach2-DFHBI	447	501	22,000	0.72	530	100
	DFHBI-1T	426	495	35,400	0.00098	-	0.22
	Spinach2-DFHBI-1T	482	505	31,000	0.94	560	184
	DFHBI-2T	460	515	34,800	0.0012	-	0.26
	Spinach2-DFHBI-2T	500	523	29,000	0.12	1300	22

[a]Extinction coefficients were all measured at pH 7.4. [b]Brightness (extinction coefficient × quantum yield) is reported relative to Spinach2—DFHBI.

in place of fluorine. For example, switching the fluorines to either bromine ((Z)-4-(3,5-dibromo-4-hydroxy-benzylidene)-1,2-dimethyl-1H-imidazol-5(4H)-one) or chlorine (Z)-4-(3,5-dichloro-4-hydroxybenzylidene)-1,2-dimethyl-1H-imidazol-5(4H)-one) resulted in compounds that bound to Spinach2 and exhibited only a slight reduction in overall fluorescence intensity compared to DFHBI (Table S1, Supporting Information (SI)). However, neither of these compounds showed a substantial shift in the peak excitation or emission wavelength when bound to Spinach2 (Table S1, Figure S1 (SI)).

We next examined if removing one fluorine would result in red-shifted fluorescence. However Spinach2 bound to ((Z)-4-(3-fluoro-4-hydroxybenzylidene)-1,2-dimethyl-1H-imidazol-5(4H)-one) again exhibited only a negligible red shift in both the excitation or emission maxima as well as a slight reduction in fluorescence because of the increased pK_a, which reduces the amount of fluorophore in the higher fluorescence phenolate form (Figure S2 (SI)). Taken together, these data indicate that fluorophores with altered halogen substituents on the benzylidene ring bind Spinach2 but do not exhibit markedly shifted spectral properties. Previous studies have shown that the HOMO—LUMO energy gap for GFP-like fluorophores is markedly influenced as the electron distribution is shifted

toward the N-1 and C-2 position.[4] The HOMO—LUMO gap directly influences the excitation and emission wavelengths of the fluorophore. We therefore tested the effects of various electron-withdrawing substituents on both positions.

We first examined the effects of substitutions at the N-1 position of the imidazolone ring. Replacing the methyl substituent in DFHBI with a 1,1,1-trifluoroethyl substituent (DFHBI-1T, (Z)-4-(3,5-difluoro-4-hydroxybenzylidene)-2-methyl-1-(2,2,2-trifluoroethyl)-1H-imidazol-5(4H)-one) resulted in a Spinach2 complex with a 35 nm red shift in the excitation peak and a slight red shift in the emission peak (Figure 1, Table 1). DFHBI-1T also exhibited an overall increase in brightness, which reflects a slight increase in the extinction coefficient and an increase in the quantum yield (Table 1).

We next tested the effect of an aminoethyl substituent at the N-1 position (DFHBI-1AE, (Z)-1-(2-aminoethyl)-4-(3,5-difluoro-4-hydroxybenzylidene)-2-methyl-1H-imidazol-5(4H)-one). At neutral pH, the aminoethyl substituent is protonated, which makes this substituent electron-withdrawing. This molecule exhibited a 30 nm red shift in the excitation and a 9 nm red shift in the emission (Figure S1, Table S1 (SI)). The overall brightness of this complex was similar to the brightness of the Spinach2 bound to DFHBI. Spinach2 bound to DFHBI-

1AE exhibited an 18% reduction in the extinction coefficient and a 24% reduction in quantum yield (Table S1 (SI)).

We also tested the effect of switching the N-1 alkyl substituent to a hydroxyl (DFHBI-1HO, (Z)-4-(3,5-difluoro-4-hydroxy-benzylidene)-1-hydroxy-2-methyl-1H-imidazol-5(4H)-one) or a methoxyl substituent (DFHBI-1MO, (Z)-4-(3,5-difluoro-4-hydroxybenzylidene)-1-methoxy-2-methyl-1H-imidazol-5(4H)-one). DFHBI-1HO exhibited markedly reduced binding to Spinach2, as well as negligible Spinach2-induced fluorescence (Table S1 (SI)). On the other hand, DFHBI-1MO exhibited only a slightly reduced binding affinity to Spinach2 (Table S1 (SI)). Spinach-DFHBI-1MO complexes were fluorescent, but did not exhibit substantial red-shifted emission. The inability of DFHBI-1HO to bind Spinach2 may reflect intramolecular hydrogen-bonding interactions between the 1-hydroxyl proton and the ketone oxygen. This may compete with interactions required for Spinach2 binding.
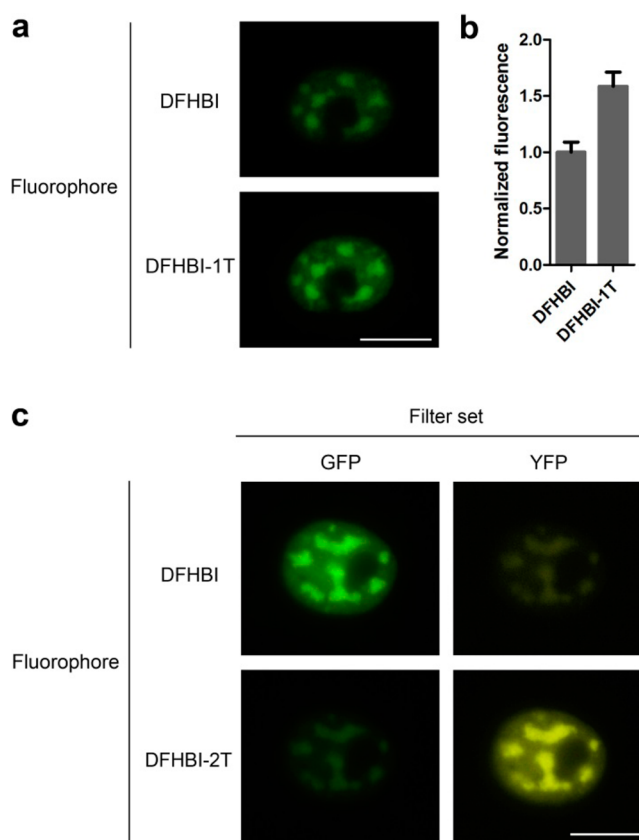
Taken together, these results suggest that N-1 alkyl substituents in the DFHBI core structure are generally well tolerated for Spinach2 binding. However, only N-1 trifluoroethyl and aminoethyl substituents caused red-shifted excitation and emission spectra.

We also considered the effects of switching the methyl substituent at the C-2 position of the imidazolinone ring to a trifluoromethyl (DFHBI-2T, (Z)-4-(3,5-difluoro-4-hydroxybenzylidene)-1-methyl-2-(trifluoromethyl)-1H-imidazol-5(4H)-one). When bound to Spinach2, this molecule exhibited a marked 53 nm red shift in the excitation and a 22 nm red shift in the emission maxima, although the overall brightness was somewhat reduced due to a decrease in the quantum yield (Figure 1, Table 1). The increase in K_D to ~1.2 μM (Figure 1, Table 1) suggests that the bulky trifluoromethyl moiety may exhibit steric hindrance with the Spinach2 aptamer.

Spinach can be engineered to form RNAs that detect small molecules in vitro.[8] In this approach, Spinach is fused to aptamers that bind to small molecules. This converts Spinach from a constitutively fluorescent complex to a fluorescent species that is allosterically regulated by small molecule binding.[8a] We asked if DFHBI-1T and DFHBI-2T enable fluorescence detection in vitro at different wavelengths than DFHBI. Indeed, incubation of the Spinach2-based S-adenosyl-methionine (SAM) sensor, composed of Spinach2 and the SAM aptamer, with each of these fluorophores resulted in SAM-dependent fluorescence emissions ranging from 501 to 523 nm (Figure S3 (SI)).

We next asked if DFHBI-1T and DFHBI-2T can be used to image Spinach2-tagged RNA in living cells. For these experiments, we expressed the CGG repeat toxic RNA that causes fragile X ataxia and tremor syndrome.[6] This RNA comprises 60 CGG repeats and forms mobile intranuclear RNA inclusions in cells. This RNA was tagged with Spinach2 as described previously.[6] Cells were initially treated with media containing 20 μM DFHBI, resulting in the expected green intranuclear foci, which were imaged using a GFP filter cube. However, replacing the media with media containing 20 μM DFHBI-1T resulted in foci that were ~60% brighter (Figure 2a,b). The increase in fluorescence is consistent with improved excitation of Spinach2 complexed with DFHBI-1T.

Additionally, we noticed that cells treated with 20 μM DFHBI-1T exhibited lower background fluorescence than cells treated with the same concentration of DFHBI. Typically DFHBI-treated cells exhibit a diffuse low-level fluorescence, even in the absence of Spinach expression (Figure S4a,b (SI)).

Figure 2. Live-cell imaging of Spinach2 fusion RNAs with different fluorophores. (a) COS7 cells expressing (CGG)$_{60}$-Spinach2 in the presence of either DFHBI or DFHBI-1T. Cells were initially cultured in the presence of 20 μM DFHBI (top panel), and images were acquired using a 100 ms exposure. The media was then exchanged with media containing 20 μM DFHBI-1T for 10 min, and images of the same cell nuclei were obtained using identical image acquisition conditions. Increased fluorescence was seen in cells cultured with DFHBI-1T (lower panel). (b) Quantification of average brightness of 10 foci normalized to brightness of DFHBI. Average and SEM values are shown. (c) Cells expressing (CGG)$_{60}$-Spinach2 in the presence of either DFHBI or DFHBI-2T were imaged using both GFP and YFP filter sets. Scale bar, 10 μm.

This fluorescence derives from the low fluorescence level of DFHBI in the media as well as faint fluorescence in cells cultured in DFHBI-containing media. Additionally, there are occasionally small fluorescent puncta in cells that reflect interactions of DFHBI with intracellular debris-like structures (Figure S4a,b (SI)). We suspect that DFHBI is weakly and nonspecifically activated by certain intracellular components. This background fluorescence is noticeable when long imaging times are used, such as when 5S-Spinach localization is imaged in cells.[5] Therefore, to image 5S-Spinach using DFHBI, the specific signal is determined by computationally subtracting the empirically measured background fluorescence, as determined by measuring the signal in cell-free portions of the image (Figure S4c (SI)). However, in DFHBI-1T-treated cells, the 5S-Spinach2 signal was readily detectable without background subtraction because of an increase in the specific fluorescence signal and because the background fluorescence was significantly lower (Figure S4 (SI)). DFHBI-1T appears to exhibit reduced nonspecific fluorescence activation by cells and in the media compared to DFHBI. Thus, Spinach2 exhibits both

higher specific fluorescence and lower background fluorescence when imaged using DFHBI-1T.

We next sought to characterize the properties of Spinach2 bound to DFHBI-2T in living cells. The spectral properties of this complex does not overlap with the standard GFP filter cube, but are instead more compatible with YFP filter cubes, which typically have an excitation bandpass filter transmitting 500 ± 10 nm light, a dichroic mirror at 515 nm, and an emission filter that transmits 535 ± 15 nm light. Indeed, cells expressing $(CGG)_{60}$-Spinach2 exhibited readily detectable intranuclear foci when imaged with the GFP filter cube, but only minimal fluorescence when imaged with the YFP filter cube (Figure 2c). However, when the media was switched with media DFHBI-2T, fluorescence was markedly reduced when imaging with the GFP filter cube but was readily detectable using the YFP filter cube (Figure 2c). These data indicate that Spinach2 imaged DFHBI-2T results in fluorescence that is detectable using the yellow emission channel.

Our studies point to the importance of substituents on the imidazolinone ring for determining the spectral emission properties of Spinach2−fluorophore complexes. These findings are consistent with previously reported studies that have extensively derivatized the GFP fluorophore.[9] In these experiments, the fluorophore was markedly influenced by substitutions on the imidazolinone ring. This portion of the fluorophore may tolerate substitutions since the Spinach aptamer was selected on agarose beads containing DFHBI connected by a linker attached at the N-1 position.[5] Thus, this position is likely to be highly tolerant of substitutions without impairing binding to Spinach2.

An important advance in this study is the identification of DFHBI-1T. DFHBI-1T exhibits lower background fluorescence than DFHBI when incubated with cells. Spinach2−DFHBI-1T exhibits increased fluorescence when imaged with GFP filter cubes due to improved excitation of the complex and lower background fluorescence. Spinach2−DFHBI-1T exhibits a Stokes shift of 23 nm compared to 54 nm for Spinach2−DFHBI. Although this smaller Stokes shift in principle requires careful selection of filter sets for imaging, the excitation and emission spectra are compatible with filter cubes commonly used to image GFP. Additionally, DFHBI-2T allows imaging of Spinach2 using the YFP filter cube. This can be valuable for experiments in which simultaneous imaging of Spinach2-tagged RNAs and CFP-tagged proteins is desired.

The different fluorophores described here provide a "plug-and-play" system for RNA imaging in living cells. The ability to alter the spectral properties of Spinach2 by using different fluorophores provides a versatility that is not seen with fluorescent proteins, which typically have fixed fluorescence properties, or in select cases can switch to a different wavelength. With a single Spinach2 construct, different spectral properties can be obtained for fluorescence imaging. Additionally, the imaging properties can be changed in a single experiment by washing out one fluorophore and adding another. This approach allows Spinach2-tagged constructs to be imaged with either GFP or YFP filter cubes. Thus, the spectral properties of Spinach2 can be matched to the specific spectral needs of the experiment. The design of Spinach2-compatible fluorophores that exhibit farther red-shifted emissions when bound to Spinach2 is a current direction for our laboratory.

■ ASSOCIATED CONTENT

Ⓢ Supporting Information

Materials and methods, details on the synthesis of small molecules, and additional figures and tables. This material is available free of charge via the Internet at http://pubs.acs.org.

■ AUTHOR INFORMATION

Corresponding Author
srj2003@med.cornell.edu

Notes
The authors declare no competing financial interest.

■ ACKNOWLEDGMENTS

■ REFERENCES

(1) Tyagi, S. *Nat. Methods* **2009**, *6*, 331−338.

(2) Bertrand, E.; Chartrand, P.; Schaefer, M.; Shenoy, S. M.; Singer, R. H.; Long, R. M. *Mol. Cell* **1998**, *2*, 437−445.

(3) Rackham, O.; Brown, C. M. *EMBO J.* **2004**, *23*, 3346−3355.

(4) (a) Babendure, J. R.; Adams, S. R.; Tsien, R. Y. *J. Am. Chem. Soc.* **2003**, *125*, 14716−14717. (b) Constantin, T. P.; Silva, G. L.; Robertson, K. L.; Hamilton, T. P.; Fague, K.; Waggoner, A. S.; Armitage, B. A. *Org. Lett.* **2008**, *10*, 1561−1564. (c) Da Costa, J. B.; Andreiev, A. I.; Dieckmann, T. *Biochemistry* **2013**, *52*, 6575−6583. (d) Sando, S.; Narita, A.; Hayami, M.; Aoyama, Y. *Chem. Commun. (Cambridge, U. K.)* **2008**, *33*, 3858−3860.

(5) Paige, J. S.; Wu, K. Y.; Jaffrey, S. R. *Science* **2011**, *333*, 642−646.

(6) Strack, R. L.; Disney, M. D.; Jaffrey, S. R. *Nat. Methods* **2013**, *10*, 1219−1224.

(7) (a) Hofer, K.; Langejurgen, L. V.; Jaschke, A. *J. Am. Chem. Soc.* **2013**, *135*, 13692−13694. (b) Pothoulakis, G.; Ceroni, F.; Reeve, B.; Ellis, T. *ACS Synth. Biol.* **2013**, DOI: 10.1021/sb400089c.

(8) (a) Paige, J. S.; Nguyen-Duc, T.; Song, W.; Jaffrey, S. R. *Science* **2012**, *335*, 1194. (b) Song, W.; Strack, R.; Jaffrey, S. R. *Nat. Methods* **2013**, *10*, 873−875. (c) Kellenberger, C. A.; Wilson, S. C.; Sales-Lee, J.; Hammond, M. C. *J. Am. Chem. Soc.* **2013**, *135*, 4906−4909. (d) Nakayama, S.; Luo, Y.; Zhou, J.; Dayie, T. K.; Sintim, H. O. *Chem. Commun. (Cambridge, U. K.)* **2012**, *48*, 9059−9061.

(9) Conyard, J.; Kondo, M.; Heisler, I. A.; Jones, G.; Baldridge, A.; Tolbert, L. M.; Solntsev, K. M.; Meech, S. R. *J. Phys. Chem. B* **2011**, *115*, 1571−1577.